ENGINEERING TRANSACTIONS • *Engng. Trans.* • **42**, 1–2, 123–143, 1994
Polish Academy of Sciences • Institute of Fundamental Technological Research

SIMPLIFIED MODEL OF ELASTIC-PLASTIC WHEEL/RAIL INTERACTIONS(*)

W. GAMBIN (WARSZAWA)

The results of numerical calculations, presented in the paper [1], demonstrate a significant role of plastic yield in the process of formation of the rail corrugations. Below, certain analytical solutions for a simplified model of wheel/rail interaction process are given. At first, normal and tangent loads of rails, assumed on the basis of the results presented in the paper [2], are analyzed. The corresponding elastic stress field is given in explicit form. Next, a complete solution for a thin, plastic surface layer of rail is proposed. The simple analytical expressions enable us to calculate the changes of *the limit shear stress* and *residual stresses* under the wheel/rail contact surface after successive passings of a wheel. Two cases are considered: a load moving with constant amplitude and a load moving with cyclically changing amplitude. Two important facts are proved. The first one – that the limit shear stress (K) and the longitudinal residual stress (R) under the running surface of rail converge to asymptotic values. The second one – that the final location of K peaks and R valleys corresponds to the positions of rail corrugations.

1. INTRODUCTION

Dynamic overloads of rail tracks lead to rail corrugations [1]. Corrugations are wave-like patterns of wavelengths 35 – 85 mm on the running surface of rails. If not controlled, they can be up to 1 mm in depth. They occur near stations where traction and breaking are heavy. Because the corrugations create an environmental noise and damage of track components, it is necessary to find a method of their elimination. Metallurgical examinations of corrugated rails indicate the formation of "white phase" – exceedingly hard material similar to martensite, which forms thin streaks about 1 cm long in the running direction. Grinding the rail, to remove corrugations, removes all signs of white phase. However, the corrugated rails and those which have been ground are prone to the rapid reappearance of corrugations.

(*) Paper supported by Grant KBN PB – 309389101, supervised by Prof. Dr. R. BOGACZ.

To explain the above phenomena, the elastic-plastic effects connected with cyclic overloads of rails are investigated in the paper. Consider a thin layer under the running surface of a rail. Two quantities determine the behaviour of the layer material: the current limit shear stress and the longitudinal component of current residual stresses. Due to dynamic overloads, the limit shear stress, uniform in new rails, increases periodically along the running surface of the exploited rails. The calculations presented below show that the places of local hardening do not move along the rails, after successive passings of the load, and can be considered as stationary. The stronger and weaker places on the running surface correspond to the position of rail corrugations. One can remove the locally hardened surface layer of rails by grinding, but this operation cannot remove the other factor which determines the rail properties – the residual stress field.

In a new rail, the residual stress field appears due to rail straightening in the manufacturing process. One can observe the tensile longitudinal component of residual stresses under the running surface of roller-straightened rails. In a working rail, the initial residual stress field undergoes certain changes. After a number of load passings, the compressive longitudinal component of residual stresses appears on the running surfaces of the rails. It will be shown later that distribution of their peaks is the same as the distribution of the lower hardening places described previously. Both the effects are complementary; however, the nature of these effects is different. Local hardening is limited to the material in *a thin layer* under the running surface of a rail. Changes of the residual stress field affect the whole cross-section of the rail. Grinding removes partially the compressive residual stresses and produces redistribution of the self-equilibriated stresses, but their variations along the running surface of the rail remain unchanged. The places on this surface with lower compressive residual stresses are subjected to formation of next corrugations.

To obtain a reasonable description of rail corrugations formation, the following problems will be considered and presented: the residual stress field in roller-straightened rails, wheel/rail contact forces – the normal and tangential ones, the elastic stress field caused by these forces, and finally, redistributions of the limit shear stresses and residual stresses in rails after successive passings of moving loads. Two cases of loads are considered: the loads moving with constant amplitude and the loads moving with amplitude cyclically changing in time. The proposed, simplified model of rail behaviour enables us to determine distributions of the critical shear stresses and the longitudinal residual stresses. Simple analytical expressions enable us to estimate the extreme values of the above quantities.

2. Residual stresses in roller-straightened rail

To obtain the straight-line shape, rails are straightened during the manufacturing process (Fig. 1).

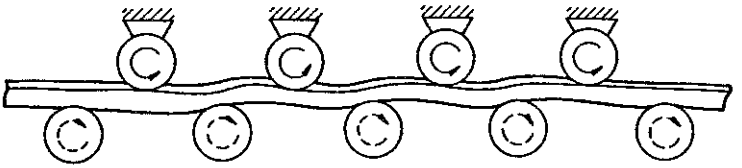

FIG. 1. Roller for rail straightening.

After straightening, the field of residual stresses appears in the rails. Distribution of the longitudinal component σ_{22}^{res}, in a cross-section of roller-straightened rail, is shown in the Fig. 2. Notice that the stress on the running surface of the rail R_0 is tensile. Its current value, in the working rail, is denoted by R.

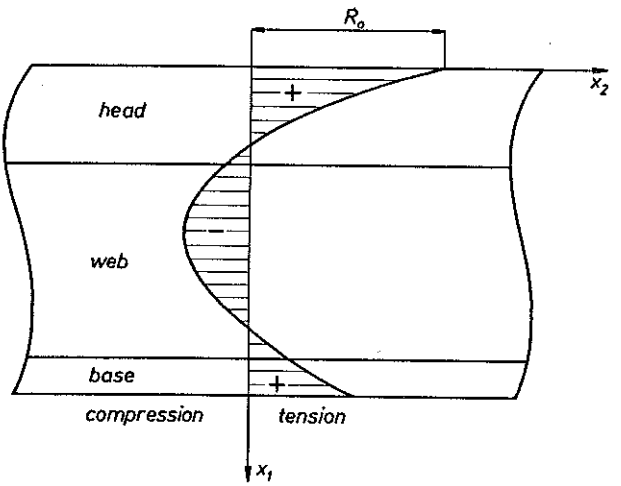

FIG. 2. Residual stress component σ_{22}^{res} in roller-straightened rail.

3. Wheel/rail contact forces

A new rail, with the initial residual stress R_0, is subjected to wheel/rail contact forces in the exploitation process. Distributions of the corresponding normal and tangent loads are given in the paper [2]. A typical load of rails is shown in the Fig. 3. Notice a complex character of the tangent load.

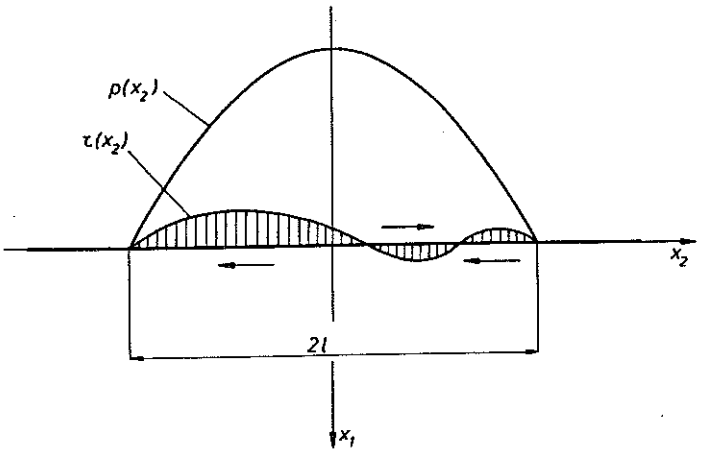

FIG. 3. Typical load of rail; $p(x_2)$ normal forces, $\tau(x_2)$ tangent forces (their directions are shown by arrows).

The quantity $2l$ in Fig. 3 denotes the contact zone width. For vertical load 200 kN caused by a wheel of the radius 900 mm, the parameter l reaches the value 10 mm [2]. Distribution of tangent forces depends on the conditions of wheel motion. A static wheel/rail interaction generates the tangent load shown in the Fig. 4a. Under the running surface of rails, such a load produces tensile longitudinal stresses during loading and compressive residual stress after unloading. This is the case of the ideal rolling contact (see [3]). For a train running with a constant speed, distribution of tangent forces is very similar to the above, and their resultant force is almost equal zero. For a heavy traction or braking of a train, distribution of tangent forces becomes similar to that shown in the Fig. 4b. Direction of the resultant force is the same as direction of the motion, in the case of braking, and the opposite when traction takes place. This is the case of ideal sliding contact.

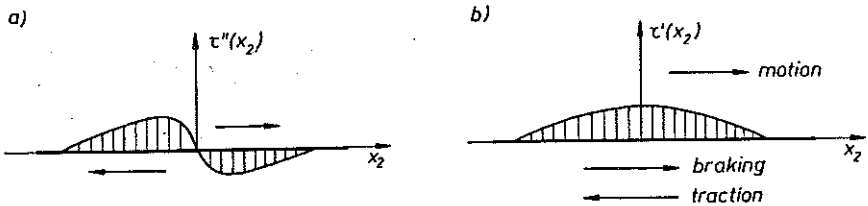

FIG. 4. Tangent load of a rail: a) ideal rolling contact, b) ideal sliding contact.

In further considerations, one can assume that the total load of rails is a superposition of three components: a) parabolic normal forces $p(x_2)$, b) parabolic tangent forces due to the sliding friction $\tau'(x_2)$, and c) tangent forces due to the rolling friction $\tau''(x_2)$, which are described by the

fifth-degree polynomial (Fig. 5):

$$p(x_2) = \frac{p_0}{l^2}\left(l^2 - x_2^2\right),$$

$$\tau(x_2) = \alpha\tau'(x_2) + (1-\alpha)\tau''(x_2), \qquad 0 \le \alpha \le 1, \tag{3.1}$$

where

$$\tau'(x_2) = \frac{\tau_0}{l^2}\left(l^2 - x_2^2\right),$$

$$\tau''(x_2) = \frac{\tau_0}{b}x_2\left(l^2 - x_2^2\right)\left(x_2^2 - a^2\right), \tag{3.2}$$

for

$$a^2 = \frac{3l^2 - 5c^2}{l^2 - 3c^2}c^2,$$

$$b^2 = \left(l^2 - c^2\right)\left(c^2 - a^2\right)c. \tag{3.3}$$

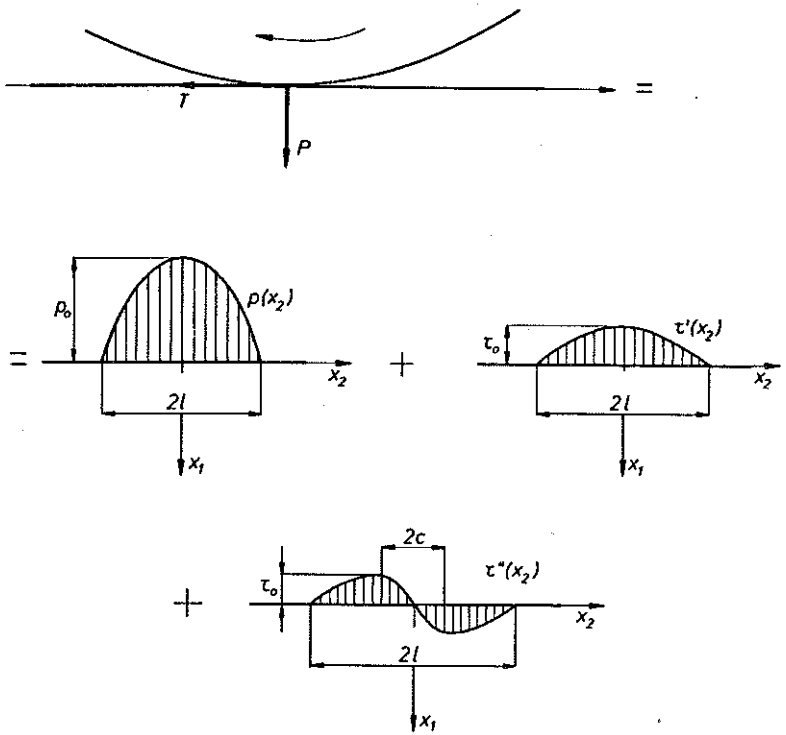

FIG. 5. Assumed decomposition of rail loads.

In the above, p_0 is the amplitude of normal forces, and τ_0 – amplitude of the tangent forces, both in the case of sliding friction and rolling friction.

The quantity $2c$ (for $c < \sqrt{3}/3$) denotes the distance between extrema of the function $\tau''(x_2)$, and depends on the wheel/rail friction conditions. It is assumed that $c = l/10$. The ratio

$$\kappa = \frac{\tau_0}{p_0} \tag{3.4}$$

describes the mentioned friction conditions and it takes values from the interval $0.1 \leq \kappa \leq 0.4$. The resultant normal and tangent forces are denoted by P and T, respectively.

4. Elastic state of rail

To determine the onset of plastic yield and to obtain the residual stress distribution in a rail, it is necessary to know the elastic stress state under the applied load. In the Appendix, the stress field, in the elastic half-space loaded by the previously described normal and tangential forces, is given. For simplicity, a piecewise linear distribution of $\tau''(x_2)$, approximating the function $(3.2)_2$, is assumed.

From the rules (A.1)–(A.8) it follows that both the onset of the plastic yield and the value of residual stresses R are determined by the value of $\sigma_{22}(x_1, x_2)$ for $x_1 = x_2 = 0$, denoted by $\sigma_{\max}$.

$$\sigma_{\max} = -p_0 + A\tau_0, \tag{4.1}$$

where

$$A = (1-\alpha)\frac{1}{\pi}\frac{l}{l-c}\ln\left(\frac{l}{c}\right)^4. \tag{4.2}$$

To introduce the compressive residual stresses R in a new rail, $\sigma_{\max}$ should be a tensile stress. It is possible when the parameter A is large enough. It takes the highest value for the case of ideal rolling contact ($\alpha = 0$). Assuming $\alpha = 0$ and $\kappa = 0.4$ (a strong friction between wheel and rail), one can obtain

$$\sigma_{\max} = 0.3025 p_0. \tag{4.3}$$

5. Plastic yield under moving load with constant amplitude

5.1. *Basic assumption*

Consider the moving load of rail shown in the Fig. 6. Let the amplitudes $p_{\max}$ and $\tau_{\max} = \kappa p_{\max}$ be large enough to cause the plastic yield of the

loaded zone. Introduce the dimensionless coordinates:

$$r = \frac{x_1}{l}, \qquad s = \frac{x_2 - \bar{x}_2}{l}, \tag{5.1}$$

where $\bar{x}_2$ is the position of the load zone center. Then, the normal and tangential forces applied are functions of $\bar{x}_2$ and s.

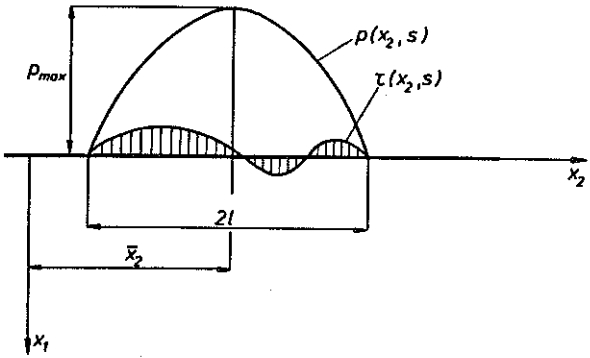

FIG. 6. Assumed moving load of rail.

For fixed $\bar{x}_2$, the applied forces are functions of the coordinate s:

$$\begin{aligned} p(s) &= p_{\max}(1 - s^2), \\ \tau(s) &= \tau_{\max}\left[\alpha(1 - s^2) + (1 - \alpha)\frac{s}{\kappa_1}(1 - s^2)(s^2 - \kappa_2)\right], \end{aligned} \tag{5.2}$$

where

$$\kappa_1 = \frac{c}{l}\left(1 - \frac{c^2}{l^2}\right)\left(1 - \frac{a^2}{l^2}\right), \qquad \kappa_2 = \frac{a^2}{l^2}. \tag{5.3}$$

The quantity a is defined by Eq. $(3.3)_1$.

The proposed analysis of plastic effects in rails is only a *static* one. It is assumed that dynamic behaviour of running trains is modelled by the moving loads acting on the rails. Inertial effects in the plastic zones are neglected. The presented approach reduces the analysis of plastic effects to the *statically determinate analysis*, i.e. the analysis expressed in terms of stress, without using any stress-strain relations. The only relation describing the plastic behaviour of rails is the Huber-Mises yield condition expressed in terms of the actual stress state and the actual limit shear stress K.

According to practical observations of the rail/wheel interactions, the normal loads may reach values, which are considerably higher than those initiating the plastic yield of the rails. To reach the proper change of K, it

is necessary to impose the following restrictions on the hardening parameter of the rail material:

1. *The hardening parameter of the rail material must be higher than a certain critical value* $h_{\min}$.

Observations show that the plastic zones are localized in thin layers under the running surface of the rails. If the hardening parameter of the rail is too large, the material cannot flow out from under the wheel and the plastic zone is of the bulk type, instead of the thin layer one. To avoid this, we assume the second restriction imposed on the hardening parameter:

2. *The hardening parameter of rail material cannot exceed a certain limit value* $h_{\max}$.

Analysis of deformation fields, for given stress-strain relations, enables us to determine $h_{\min}$ and $h_{\max}$, but it is not the subject of the paper. Our purpose is to find the changes of K and R due to the applied loads, under the restrictions 1 and 2. The following basic assumption is taken:

Due to the applied load, plastic yielding occurs in a thin layer under the running surface of rails. The shear stress component does not change through the layer thickness.

The basic assumption yields

$$\sigma_{rs} = \sigma_{rs}(s). \tag{5.4}$$

5.2. Basic solution

Introducing the boundary conditions

$$\sigma_{rr}(s) = -p(s), \qquad \sigma_{rs}(s) = -\tau(s), \tag{5.5}$$

and the restrictions (5.4) into the equilibrium equations

$$\begin{aligned} \sigma_{rr,r} + \sigma_{rs,s} &= 0, \\ \sigma_{ss,s} + \sigma_{rs,r} &= 0, \end{aligned} \tag{5.6}$$

one can obtain the following solution:

$$\begin{aligned} \sigma_{rr}(r,s) &= -p(s) + \frac{d\tau(s)}{ds} r, \\ \sigma_{ss}(s) &= C_1 = \text{const}, \\ \sigma_{rs}(s) &= -\tau(s). \end{aligned} \tag{5.7}$$

Notice that σ_{rr} varies linearly across the layer thickness, σ_{ss} has the same value C_1 in the whole plastic zone, and σ_{rs} does not change its value across the layer thickness.

The value C_1 can be determined from the elastic solution. Denote by $\overline{p}$ and $\overline{\tau}$ the amplitudes of $p(s)$ and $\tau(s)$, respectively, under which the onset of plastic yield occurs. Let $\overline{\sigma}_{\max}$ be the corresponding value of $\sigma_{22}(0,0)$ in the elastic state. Then

$$C_1 = \overline{\sigma}_{\max} + R, \tag{5.8}$$

where R is the longitudinal component of the current residual stress at the point in which the plastic yield occurs. Taking into account Eq. (4.1), one can finally write

$$C_1 = -\kappa\overline{\tau} + A\overline{\tau} + R. \tag{5.9}$$

In the plastic zone the following Huber-Mises yield criterion should be satisfied:

$$(\sigma_{ss} - \sigma_{rr})^2 + 4\sigma_{rs}^2 = 4K^2. \tag{5.10}$$

The quantity K is an unknown, current shear stress limit.

To determine $\overline{\tau}$, R and K, consider the plastic yield onset in a new rail after *the first* passing of the load. It takes place on the running surface of the rail ($r = 0$), at the point $s = 0$. Then $\overline{\tau}$, $\overline{p}$, R and K take values $\overline{\tau}_1$, $\overline{p}_1$, R_0 and K_0, respectively, where the values R_0 and K_0 are known. According to Eq. (5.7), the stress state at point $s = 0$ is the following:

$$\begin{aligned} \sigma_{rr}(0,0) &= -\overline{\kappa}\tau_1, \\ \sigma_{ss}(0) &= -\kappa\overline{\tau}_1 + A\overline{\tau}_1 + R_0, \\ \sigma_{rs}(0) &= -\overline{\tau}_1. \end{aligned} \tag{5.11}$$

Introducing Eq. (5.10) into Eq. (5.9), with K equal to K_0, one can determine the amplitude of tangential forces which causes the plastic yield

$$\overline{\tau}_1 = \frac{-AR_0 + [A^2R_0^2 + (A^2 + 4\alpha^2)(4K_0^2 - R_0^2)]^{1/2}}{A^2 + 4\alpha^2}, \tag{5.12}$$

or the corresponding amplitude of normal forces:

$$\overline{p}_1 = \overline{\tau}_1/\kappa. \tag{5.13}$$

Concluding, the stress field in the plastic zone on the running surface of a new rail after *the first* passing of the load is the following:

$$
\begin{aligned}
&\sigma_{rr}(s,0) = p_{\max}^2(s-1),\\
&\sigma_{ss}(s) = \overline{\tau}_1\left(A-\frac{1}{\kappa}\right)+R_0,\\
&\sigma_{rs}(s) = p_{\max}\kappa(s^2-1)\left[\alpha(1-\alpha)\frac{s}{\kappa_1}(s^2-\kappa_2)\right],
\end{aligned}
\tag{5.14}
$$

for $p_{\max} \geq \overline{\tau}_1/\kappa$.

5.3. *Change of the limit shear stress after successive passings*

Introducing the solution (5.14) into the yield criterion (5.10), one can obtain the value of K in a new rail after *the first* passing of the load. Repeating the calculations, one can find the limit shear stress $K_{(i)}$ after *the i-th* passing of the load with amplitude $p_{\max}^{(i)} \geq \overline{\tau}_{(i)}/\kappa$:

$$
K_{(i)} = \frac{1}{2}\left\{\left[p_{\max}^{(i)}+\left(A-\frac{1}{\kappa}\right)\overline{\tau}_{(i)}+R_{(i-1)}\right]^2+\left(2\frac{\alpha}{\kappa}p_{\max}^{(i)}\right)^2\right\}^{1/2},
\tag{5.15}
$$

where

$$
\tau_{(i)} = \frac{-AR_{(i-1)}+\left[A^2R_{(i-1)}^2+(A^2+4\alpha^2)\left(4K_{(i-1)}^2-R_{(i-1)}^2\right)\right]^{1/2}}{A^2+4\alpha^2},
\tag{5.16}
$$

for $i = 1,2,3,\ldots$ and $K_{(0)} = K_0$, $R_{(0)} = R_0$, $\overline{\tau}_{(1)} = \overline{\tau}_1$.

In the above rules, $R_{(i-1)}$ should be determined for each step of calculations.

5.4. *Change of residual stresses*

After *the i-th* passing of the load $p_{\max}^{(i)} \geq \overline{\tau}_{(i)}/\kappa$, residual stresses can be determined from the general rule:

$$
R_{(i)} = \sigma_{ss}^{(i)} - \overline{\sigma}_{\max}^{(i)},
\tag{5.17}
$$

where $\sigma_{ss}^{(i)}$ and $\overline{\sigma}_{\max}^{(i)}$ are the appropriate stress components in plastic and elastic state, respectively. According to $(5.14)_2$ and (4.1), one can write

$$
\begin{aligned}
&\sigma_{ss}^{(i)} = \overline{\tau}_{(i)}\left(A-\frac{1}{\kappa}\right)+R_{(i-1)},\\
&\overline{\sigma}_{\max}^{(i)} = p_{\max}^{(i)}(A\kappa-1).
\end{aligned}
\tag{5.18}
$$

Then

$$R_{(i)} = R_{(i-1)} + \left(A - \frac{1}{\kappa}\right)\left(\overline{\tau}_{(i)} - \kappa p^{(i)}_{\max}\right). \tag{5.19}$$

The rules (5.15), (5.16) and (5.19) fully describe the considered problem, for the case of a load moving with a constant amplitude.

5.5. Some calculations

Apply the above results to the analysis of plastic effects caused by typical wheel/rail interactions. According to the data of BHP Steel International Group [4], a mean wheel load P is taken as 200 kN – 300 kN, the initial limit shear stress $K_0 = 500\,\text{MPa}$, and residual stress in roller straightened rail $R_0 = 40\,\text{MPa}$. Taking $l = 10\,\text{mm}$, $c = 1\,\text{mm}$, a wheel/rail contact area as $200\,\text{mm}^2$, and $\kappa = 0.4$, one can calculate the following amplitudes of the normal contact forces $p_{\max}$: 750 MPa, 938 MPa and 1125 MPa, for the resulting loads P equal to 200 kN, 250 kN and 300 kN, respectively. If we assume the case of heavy traction or braking of the train, then $\alpha = 0$, and the rule (5.16) is reduced to the following relation:

$$\overline{\tau}_{(i)} = \frac{1}{A}\left(2K_{(i-1)} - R_{(i-1)}\right). \tag{5.20}$$

Then

$$\begin{aligned} K_{(i)} &= \frac{1}{2}p^{(i)}_{\max} + \left(1 - \frac{1}{A\kappa}\right)K_{(i-1)} + \frac{1}{2A\kappa}R_{(i-1)}, \\ R_{(i)} &= (1 - A\kappa)p^{(i)}_{\max} + 2\left(1 - \frac{1}{A\kappa}\right)K_{(i-1)} + \frac{1}{A\kappa}R_{(i-1)}. \end{aligned} \tag{5.21}$$

Consider a series of successive passings of the same load P applied to a new rail. Then, the above rules give the following results, which are valid for $i = 1, 2, 3, \ldots$:

$$\begin{aligned} K_{(i)} &= 507\,\text{MPa}, \quad R_{(i)} = 36\,\text{MPa}, \quad \text{when} \quad P = 200\,\text{kN}, \\ K_{(i)} &= 601\,\text{MPa}, \quad R_{(i)} = -21\,\text{MPa}, \quad \text{when} \quad P = 250\,\text{kN}, \\ K_{(i)} &= 694\,\text{MPa}, \quad R_{(i)} = -78\,\text{MPa}, \quad \text{when} \quad P = 300\,\text{kN}. \end{aligned}$$

Notice that for each of the considered cases, K and R take their final values after the first passing of the load. For a series of passings with the increasing loads, i.e.: $P_{(1)} = 200\,\text{kN}$, $P_{(2)} = 250\,\text{kN}$ and $P_{(i)} = 300\,\text{kN}$ (for $i = 3, 4, 5, \ldots$), the successive results are the same.

Sometimes, due to the rail technology used, the initial residual stress R_0 is much more higher than the assumed one. Consider the last series of passings for the increasing loads applied to a new rail with $R_0 = 120\,\text{MPa}$. Then

$$K_{(1)} = 537\,\text{MPa}, \quad R_{(1)} = 97\,\text{MPa}, \quad \text{when} \quad P = 200\,\text{kN},$$
$$K_{(2)} = 631\,\text{MPa}, \quad R_{(2)} = 40\,\text{MPa}, \quad \text{when} \quad P = 250\,\text{kN},$$
$$K_{(i)} = 725\,\text{MPa}, \quad R_{(i)} = -16\,\text{MPa}, \quad \text{when} \quad P = 300\,\text{kN},$$

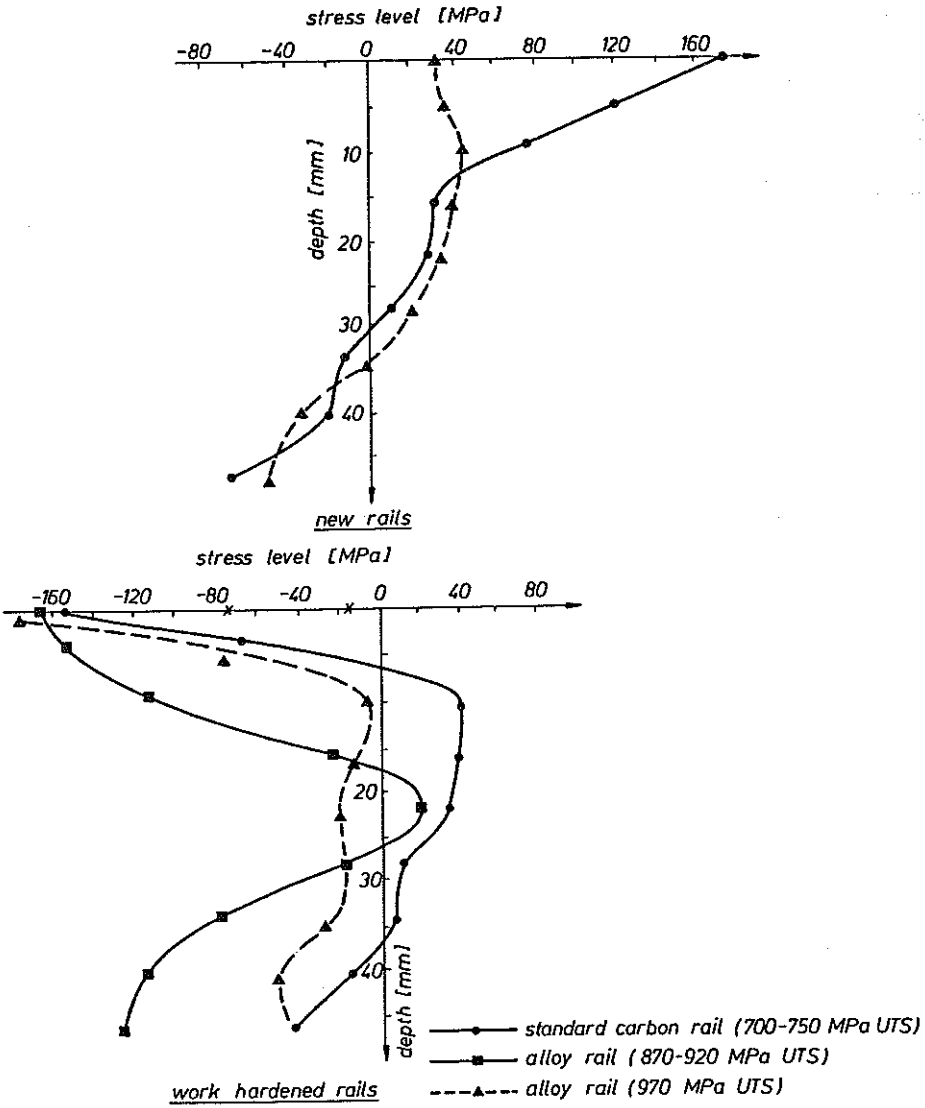

FIG. 7. Redistribution of longitudinal residual stress in rail (after MAIR and GROENHOUT [4]).

for $i = 3, 4, 5, \ldots$. Following [4], the results of tests for standard carbon and alloy rails are shown in the Fig. 7. Notice a qualitative agreement of the presented calculations (crosses in the right-hand part of the Fig. 7) with the referred tests.

6. Plastic yield under moving load with cyclically changing amplitude

The most significant factor determining formation of corrugations is rail vibration under the action of a moving and oscillating load [1]. It means that our analysis should take into account loads cyclically changing during their motion. The load oscillations may be described by smooth harmonic functions. However, the analysis based on such functions leads to very complex relations. For this reason, we assume the load variation as that shown in the Fig. 8.

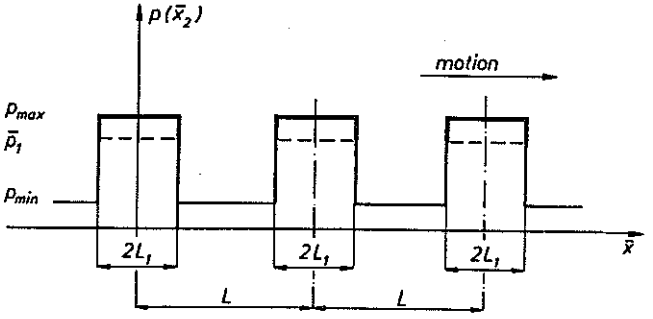

Fig. 8. Moving and oscillating load of a rail.

Because the considered load moves at a constant rate, one can regard the load variation as a function of position of the contact zone center $\overline{x}_2$. Then, the amplitude of the normal forces has the following form:

$$p_c(\overline{x}_2) = \begin{cases} p_{\max} & \text{for} \quad -L_1 + nL \leq \overline{x}_2 \leq L_1 + nL, \\ p_{\min} & \text{for} \quad L_1 + nL \leq \overline{x}_2 \leq -L_1 + (n+1)L, \end{cases} \tag{6.1}$$

where $n = 0, \mp 1, \mp 2, \ldots$, L and L_1 are shown in the Fig. 8.

The amplitude of tangential forces $\tau_c(\overline{x}_2)$ is described by the same function with values $\tau_{\max}$ and $\tau_{\min}$, instead of $p_{\max}$ and $p_{\min}$, respectively. The values $\overline{p}_1$ and $\overline{\tau}_1$ correspond to the plastic yield onset. In the dimensionless system of coordinates $\{r, s\}$ (see Sec. 5.1), distributions of the normal and tangential loads, $p(\overline{x}_2, s)$ and $\tau(\overline{x}_2, s)$, are given by the rules (5.2), in which $p_c(\overline{x}_2)$ and $\tau_c(\overline{x}_2)$ are taken instead of $p_{\max}$ and $\tau_{\max}$, respectively. It is assumed that all the dynamic wheel/rail interactions caused by inertia forces are taken into account through the normal and tangential load. However,

the inertial effects in the plastic zone, because of the negligible small mass of the plastic layer, are not considered.

Repeat the analysis presented in Sec. 5.2. Consider the stress field components: $\sigma_{rr}(\overline{x}_2, s)$, $\sigma_{ss}(\overline{x}_2, s)$ and $\sigma_{rs}(\overline{x}_2, s)$, in the plastic zone on the running surface of a new rail. It easy to see that, after *the first* passing of the cyclically changing load, these components are given by the rules (5.14), in which $p_c(\overline{x}_2)$ and $\tau_c(\overline{x}_2)$ are taken instead of $p_{\max}$ and $\tau_{\max}$, respectively. Cyclic oscillations of loads lead to nonuniform fields: $\overline{\tau}_1(\overline{x}_2)$, $K(\overline{x}_2)$ and $R(\overline{x}_2)$. For simplicity, the argument $\overline{x}_2$ will be omitted in further considerations. To obtain the above fields, one can use the rules (5.15), (5.16) and (5.19) with certain modifications. Notice that the rules (5.15), (5.16) and (5.19), applied to the cyclic loads, lead to stepwise distribution of K and R. The real distributions of K and R are smooth at the ends of step intervals. Moreover, τ and R in the considered rules should determine the constant C_1 in the rule (5.9). This constant was derived for the case of the initial plastic yield. Then, τ and R must be taken *at the fronts of plastic zones.* However, the residual stresses R, generated by the thin plastic layers, are partly taken over by the adjacent elastic zones. Then, R takes a certain mean value between that in the plastic zone and that in the elastic one. Denote by $\overline{\tau}^f_{(i)}$ and $R^f_{(i)}$ the values of $\overline{\tau}_{(i)}$ and $R_{(i)}$ at the fronts of plastic zones. If the distance L is not too large, it is reasonable to assume that

$$R^f_{(i)} = \frac{1}{2}\left(R^{f-}_{(i)} + R^{f+}_{(i)}\right), \tag{6.2}$$

where $R^{f-}_{(i)}$ and $R^{f+}_{(i)}$ are values of $R_{(i)}$ at the points of discontinuity.

Following the rules (5.15) and (5.16), one can obtain the limit of shear stress after *the i-th* passing of the load:

$$K_{(i)} = \left\{\left[p^{(i)}_{\max} + \left(A - \frac{1}{\kappa}\right)\overline{\tau}^f_{(i)} + R^f_{(i-1)}\right]^2 + \left(2\frac{\alpha}{\kappa}p^{(i)}_{\max}\right)^2\right\}^{1/2} \tag{6.3}$$

in plastically deformed zones, when $p^{(i)}_{\max} \geq \overline{p}_{(i)} = \kappa\overline{\tau}^f_{(i)}$, and $K_{(i)} = K_{(i-1)}$ in the remaining zones of rail surface layer. The quantity $\overline{\tau}^f_{(i)}$ is calculated from the relation

$$\overline{\tau}^f_{(i)} = \frac{-AR^f_{(i-1)}}{A^2 + 4\alpha^2} + \frac{\left\{A^2\left(R^f_{(i-1)}\right)^2 + (A^2 + 4\alpha^2)\left[4K^2_{(i-1)} - \left(R^f_{(i-1)}\right)^2\right]\right\}^{1/2}}{A^2 + 4\alpha^2}. \tag{6.4}$$

The corresponding residual stresses may be estimated on the basis of the rule (cf. Eq. (5.19)):

$$R_{(i)} = R^f_{(i-1)} + \left(A - \frac{1}{\kappa}\right)\left[\overline{\tau}^f_{(i)} - \kappa p^{(i)}_{\max}\right]. \tag{6.5}$$

Observe that the relations (6.2)–(6.5) fully describe the considered problem.

For $\alpha = 0$, the following rules may be used:

$$\begin{aligned} K_{(i)} &= \frac{1}{2}p^{(i)}_{\max} + \left(1 - \frac{1}{A\kappa}\right)K_{(i-1)} + \frac{1}{2A\kappa}R^f_{(i-1)}, \\ \overline{\tau}^f_{(i)} &= \frac{1}{A}\left(2K_{(i-1)} - R^f_{(i-1)}\right), \\ R_{(i)} &= (1 - A\kappa)p^{(i)}_{\max} + 2\left(1 - \frac{1}{A\kappa}\right)K_{(i-1)} + \frac{1}{A\kappa}R^f_{(i-1)}. \end{aligned} \tag{6.6}$$

Now, consider a series of successive passings of the same cyclically changing load with amplitudes shifted by the distance $L_1 + L$ (see Fig. 9). Assume the same data as in Sec. 5.5, i.e.: the initial limit shear stress $K_0 = 500\,\mathrm{MPa}$, the initial residual stress $R_0 = 40\,\mathrm{MPa}$, $l = 10\,\mathrm{mm}$, $c = 1\,\mathrm{mm}$, the wheel/rail contact area – $200\,\mathrm{mm}^2$ and $\kappa = 0.4$. For the maximum load P equal to 300 kN and the case $\alpha = 0$, the rules (6.6) lead to the following results (see also Fig. 9):

$$\begin{aligned}
&K_{(1)}(\overline{x}_2) = 694\,\mathrm{MPa}, \quad R_{(1)}(\overline{x}_2) = -78\,\mathrm{MPa} \\
&\qquad\qquad \text{for} \quad (4n-1)L_1 \le \overline{x}_2 \le (4n+1)L_1, \\
&K_{(1)}(\overline{x}_2) = 500\,\mathrm{MPa}, \quad R_{(1)}(\overline{x}_2) = 40\,\mathrm{MPa} \\
&\qquad\qquad \text{for} \quad (4n+1)L_1 \le \overline{x}_2 \le (4n+3)L_1, \\
&K_{(2)}(\overline{x}_2) = 694\,\mathrm{MPa}, \quad R_{(2)}(\overline{x}_2) = -78\,\mathrm{MPa} \\
&\qquad\qquad \text{for} \quad (4n-1)L_1 \le \overline{x}_2 \le (4n+1)L_1, \\
&K_{(2)}(\overline{x}_2) = 671\,\mathrm{MPa}, \quad R_{(2)}(\overline{x}_2) = -123\,\mathrm{MPa} \\
&\qquad\qquad \text{for} \quad (4n+1)L_1 \le \overline{x}_2 \le (4n+3)L_1, \\
&K_{(3)}(\overline{x}_2) = 694\,\mathrm{MPa}, \quad R_{(3)}(\overline{x}_2) = -78\,\mathrm{MPa} \\
&\qquad\qquad \text{for} \quad (4n-1)L_1 \le \overline{x}_2 \le (4n+1)L_1, \\
&K_{(3)}(\overline{x}_2) = 671\,\mathrm{MPa}, \quad R_{(3)}(\overline{x}_2) = -123\,\mathrm{MPa} \\
&\qquad\qquad \text{for} \quad (4n+1)L_1 \le \overline{x}_2 \le (4n+3)L_1, \\
&K_{(i)}(\overline{x}_2) = 694\,\mathrm{MPa}, \quad R_{(i)}(\overline{x}_2) = -78\,\mathrm{MPa} \\
&\qquad\qquad \text{for} \quad (4n-1)L_1 \le \overline{x}_2 \le (4n+1)L_1, \\
&K_{(i)}(\overline{x}_2) = 680\,\mathrm{MPa}, \quad R_{(i)}(\overline{x}_2) = -106\,\mathrm{MPa} \\
&\qquad\qquad \text{for} \quad (4n+1)L_1 \le \overline{x}_2 \le (4n+3)L_1,
\end{aligned}$$

for $i = 4, 5, 6, \ldots$.

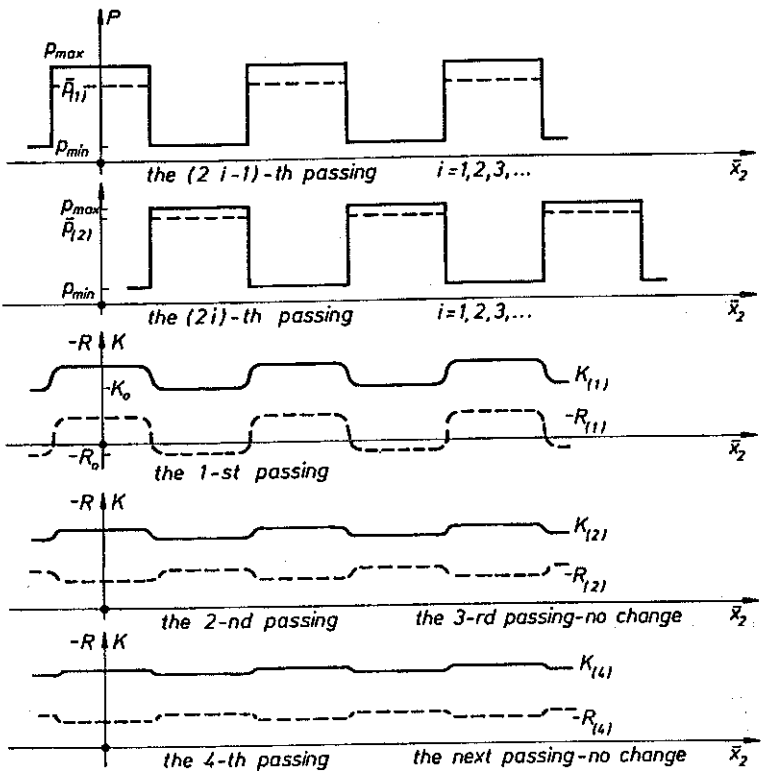

FIG. 9. Distribution of critical shear stress and residual stresses after successive passings of loads with shifted amplitudes.

The results of calculations show that, after the second passing, the hardening of the plastically deformed zones is smaller than after the first one, but the introduced compressive stresses are higher. The situation does not change after subsequent passings. It means that the peaks of residual stresses are situated at the weaker places of rail. The places of local hardening and highest residual stresses do not move along the rails after successive passings of cyclically changing loads.

Notice that after the third, fifth and next passings, no plastic zones occur on the running surface of rail. It means that the limit shear stress and the longitudinal residual stress take their ultimate values after a number of passings.

7. CONCLUSIONS

The presented analysis proves that elastic-plastic effects due to dynamic

wheel/rail interactions are responsible for formation of the rail corrugations. Cyclically changing moving loads cause a heterogeneity of distribution of both the hardening of material and the residual stresses in rails. Magnitude of local hardening and residual stresses become stabilized after a few passings of the load. Places of lower hardening correspond to the positions of peaks of the residual stresses on the running surface of rails. The considered places do not move along the rails after successive passings of the load and indicate the positions of rail corrugations.

Notice that only the highest loads influence the rail properties. A high load with constant amplitude applied to a new rail may delay formation of the rail corrugations. Such a load generates a uniform, strong hardening of the material and uniformly distributed, compressive residual stresses on the running surface of the rail. Both the factors protect the rails against the effects of dynamic overloading.

Finally, it is necessary to point out that the problems of rail technology are close to those which appear during the treatment processes of metal surface layers in tools and machine elements. Some micromechanical investigations of a metal surface layer behaviour may be successfully applied in the design of the running surfaces of rails. Particularly, the texture development analysis [5] enables us to take into account the influence of the advanced plastic yield on the surface layer properties.

APPENDIX. STRESS STATE OF ELASTIC HALF-SPACE

Consider an elastic half-space under the normal and tangential loads given by the rules (3.1) and (3.2). Divide them into two groups: a) the parabolic loads with amplitudes p_0 and τ_0 (Fig. 10), b) the piece-linear load which is an approximation of the fifth degree polynomial $(3.2)_2$ (Fig. 11). The first group of loads generates the stress field $\sigma'(x_1, x_2)$, the second – $\sigma''(x_1, x_2)$. The total stress field $\sigma(x_1, x_2)$ is the sum of the above ones. To obtain the field $\sigma(x_1, x_2)$, the standard Green's function approach is used.

Introduce the notations (Fig. 10):

$$\sin\Theta_{1,2} = \frac{x_2 \mp l}{r_{1,2}}, \qquad \cos\Theta_{1,2} = \frac{x_1}{r_{1,2}}, \tag{A.1}$$

where

$$r_{1,2} = \sqrt{x_1^2 + (x_2 \mp l)^2}. \tag{A.2}$$

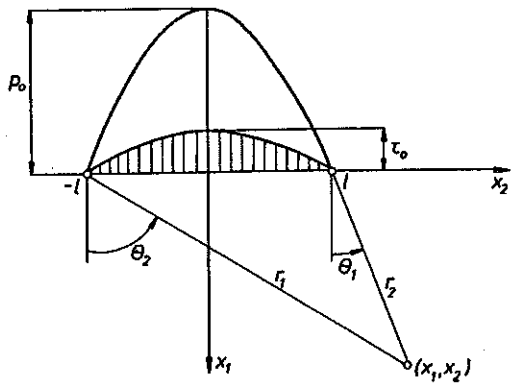

FIG. 10. Elastic half-space under parabolic loads.

The solution of the considered problem for parabolic loads is the following:

$$\text{(A.3)}\qquad \sigma'_{11}(x_1,x_2) = 2\frac{p_0}{\pi l^2}\left\{\frac{x_1^2}{4}[\sin 2\Theta_1 - \sin 2\Theta_2 + 2(\Theta_2-\Theta_1)]\right.$$
$$\left. -\frac{x_1x_2}{2}(\cos 2\Theta_1 - \cos 2\Theta_2) + \frac{x_2^2-l^2}{4}[\sin 2\Theta_2 - \sin 2\Theta_1 + 2(\Theta_2-\Theta_1)]\right\}$$
$$-2\frac{\tau_0}{\pi l^2}\alpha\left\{\frac{x_1^2}{4}\left[\cos 2\Theta_2 - \cos 2\Theta_1 + \ln\left(\frac{r_2}{r_1}\right)^4\right]\right.$$
$$-\frac{x_1x_2}{4}[(\sin 2\Theta_1 - \sin 2\Theta_2) + 2(\Theta_2-\Theta_1)]$$
$$\left. +\frac{x_2^2-l^2}{4}(\cos 2\Theta_1 - \cos 2\Theta_2)\right\},$$

$$\text{(A.4)}\qquad \sigma'_{22}(x_1,x_2) = 2\frac{p_0}{\pi l^2}\left\{2x_1l + \frac{x_1^2}{4}[\sin 2\Theta_2 - \sin 2\Theta_1 + 6(\Theta_1-\Theta_2)]\right.$$
$$-\frac{x_1x_2}{2}\left[\cos 2\Theta_2 - \cos 2\Theta_1 + \ln\left(\frac{r_2}{r_1}\right)^4\right]$$
$$\left. +\frac{x_2-l^2}{4}[\sin 2\Theta_1 - \sin 2\Theta_2 + 2(\Theta_2-\Theta_1)]\right\}$$
$$-2\frac{\tau_0}{\pi l^2}\alpha\left\{2x_1l + \frac{x_1^2}{4}\left[\cos 2\Theta_1 - \cos 2\Theta_2 - \ln\left(\frac{r_2}{r_1}\right)^8\right] - 4x_2l\right.$$
$$-\frac{x_1x_2}{2}[\sin 2\Theta_2 - \sin 2\Theta_1 + 6(\Theta_2-\Theta_1)]$$
$$\left. +\frac{x_2^2-l^2}{2}\left[\cos 2\Theta_2 - \cos 2\Theta_1 - \ln\left(\frac{r_2}{r_1}\right)^4\right]\right\},$$

$$(A.5)\qquad \sigma'_{12}(x_1,x_2)=2\frac{p_0}{\pi l^2}\left\{\frac{x_1^2}{4}\left[\cos 2\Theta_2-\cos 2\Theta_1+\ln\left(\frac{r_2}{r_1}\right)^4\right]\right.$$
$$\left.-\frac{x_1x_2}{2}\left[\sin 2\Theta_1-\sin 2\Theta_2+2(\Theta_2-\Theta_1)\right]+\frac{x_2-l^2}{4}\left(\cos 2\Theta_1-\cos 2\Theta_2\right)\right\}$$
$$-2\frac{\tau_0}{\pi l^2}\alpha\left\{2x_1l+\frac{x_1^2}{4}\left[\sin 2\Theta_2-\sin 2\Theta_1+6(\Theta_2-\Theta_1)\right]\right.$$
$$-\frac{x_1x_2}{2}\left[\cos 2\Theta_2-\cos 2\Theta_1+\ln\left(\frac{r_2}{r_1}\right)^4\right]$$
$$\left.+\frac{x_2^2-l^2}{2}\left[\sin 2\Theta_1-\sin 2\Theta_2+2(\Theta_2-\Theta_1)\right]\right\},$$

The piecewise linear load is decomposed into three linear parts: $\tau_1(x_2)$, $\tau_2(x_2)$ and $\tau_3(x_2)$ (Fig. 11), where

$$(A.6)\qquad \tau_{1,3}(x_2)=\frac{\tau_0}{l-c}(x_2\mp l),\qquad \tau_2(x_2)=\frac{\tau_0}{c}x_2.$$

According to the rules (A.1), introduce the coordinates $\{r'_{1,2},\Theta'_{1,2}\}$, $\{r''_{1,2},\Theta''_{1,2}\}$ and $\{r'''_{1,2},\Theta'''_{1,2}\}$ in the intervals $\{-l,-c\}$, $\{-c,c\}$ and $\{c,l\}$, respectively.

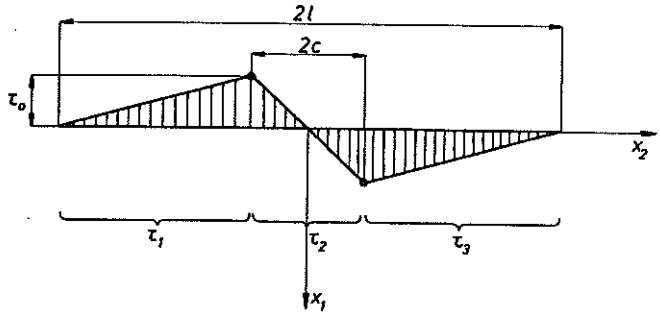

FIG. 11. Elastic half-space under piecewise linear load.

The solution of the considered problem for a piecewise linear load is the following:

$$(A.7)\qquad \sigma''_{11}(x_1,x_2)=-\frac{2\tau_0}{\pi c(l-c)}(1-\alpha)\left\{\frac{x_1c}{4}\left[\sin 2\Theta'_1-\sin 2\Theta'_2\right.\right.$$
$$\left.+2(\Theta'_2-\Theta'_1)\right]-\frac{(x_2+l)c}{4}\left(\cos 2\Theta'_1-\cos 2\Theta'_2\right)$$
$$-\frac{x_1(l-c)}{4}\left[\sin 2\Theta''_1-\sin 2\Theta''_2+2(\Theta''_2-\Theta''_1)\right]$$

(A.7) [cont.]

$$+\frac{x_2(l-c)}{4}(\cos 2\Theta_1'' - \cos 2\Theta_2'')$$
$$+\frac{x_1 c}{4}\left[\sin 2\Theta_1''' - \sin 2\Theta_2''' + 2(\Theta_2''' - \Theta_1''')\right]$$
$$-\frac{(x_2-l)c}{4}(\cos 2\Theta_1' - \cos 2\Theta_2')\Big\}.$$

(A.8)
$$\sigma_{22}''(x_1,x_2) = -\frac{2\tau_0}{\pi c(l-c)}(1-\alpha)\Big\{-1+\frac{x_1 c}{4}\left[\sin 2\Theta_2' - \sin 2\Theta_1'\right.$$
$$\left.+6(\Theta_1' - \Theta_2')\right] - \frac{(x_2+l)c}{4}\left[\cos 2\Theta_2' - \cos 2\Theta_1' + \ln\left(\frac{r_2'}{r_1'}\right)^4\right]$$
$$-\frac{x_1(l-c)}{4}\left[\sin 2\Theta_2'' - \sin 2\Theta_1'' + 6(\Theta_1'' - \Theta_2'')\right]$$
$$+\frac{x_2(l-c)}{4}\left[\cos 2\Theta_2'' - \cos 2\Theta_1'' + \ln\left(\frac{r_2''}{r_1''}\right)^4\right]$$
$$+\frac{x_1 c}{4}\left[\sin 2\Theta_2''' - \sin 2\Theta_1''' + 6(\Theta_1''' - \Theta_2''')\right]$$
$$-\frac{(x_2-l)c}{4}\left[\cos 2\Theta_2' - \cos 2\Theta_1' + \ln\left(\frac{r_2'''}{r_1'''}\right)^4\right]\Big\}$$

(A.9)
$$\sigma_{12}''(x_1,x_2) = -\frac{2\tau_0}{\pi c(l-c)}(1-\alpha)\Big\{\frac{x_1 c}{4}\left[\cos 2\Theta_2' - \cos 2\Theta_1' + \ln\left(\frac{r_2'}{r_1'}\right)^4\right]$$
$$-\frac{(x_2+l)c}{4}\left[\sin 2\Theta_1' - \sin 2\Theta_2' + 2(\Theta_2' - \Theta_1')\right]$$
$$-\frac{x_1(l-c)}{4}\left[\cos 2\Theta_2'' - \cos 2\Theta_1'' + \ln\left(\frac{r_2''}{r_1''}\right)^4\right]$$
$$+\frac{x_2(l-c)}{4}\left[\sin 2\Theta_1'' - \sin 2\Theta_2'' + 2(\Theta_2'' - \Theta_1'')\right]$$
$$+\frac{x_1 c}{4}\left[\cos 2\Theta_2''' - \cos 2\Theta_1''' + \ln\left(\frac{r_2'''}{r_1'''}\right)^4\right]$$
$$-\frac{(x_2-l)c}{4}\left[\sin 2\Theta_1''' - \sin 2\Theta_2''' + 2(\Theta_2''' - \Theta_1''')\right]\Big\}.$$

Acknowledgement. The author is very grateful to Dr. B. GAMBIN for fruitful discussions and helpful suggestions.

REFERENCES

1. R. BOGACZ, *On residual stresses in rails and wheel/rail interaction; in Residual Stresses in Rails*, vol. **2**, Kluwer Academic Publishers, 1992.
2. M. BRZOZOWSKI, R. BOGACZ and K. POPP, *Zur Reibungsmodellierung beim Rollkontakt*, ZAMM, **70**, 6, T 678 – T 679, 1990.
3. K.L. JOHNSON, *Contact mechanics*, Cambridge University Press, 1985.
4. R. MAIR and R. GROENHOUT, *The growth of transverse fatigue defects in head of railway rails*, [in:] Rail Research Papers; Compendium of BHP Steel International Group, vol. **1**, Melbourne 1980.
5. W. GAMBIN, A. NAKONIECZNY, K. SKALSKI, *Original and strain induced plastic anisotropy in metal surface layers*, J. Theor. Appl. Mech., **31**, 4, 1993.

POLISH ACADEMY OF SCIENCES
INSTITUTE OF FUNDAMENTAL TECHNOLOGICAL RESEARCH.

Received November 10, 1993.